applied sciences

MDPI

Article

Development of Energy Management Systems for Electric Vehicle Charging Stations Associated with Batteries: Application to a Real Case

Jon Olano [1], Haritza Camblong [1,2,*], Jon Ander López-Ibarra [3] and Tek Tjing Lie [2]

[1] Department of Systems Engineering & Control, Faculty of Engineering of Gipuzkoa, University of the Basque Country (UPV-EHU), Europa Plaza 1, CP 20018 Donostia, Spain; jon.olanoa@ehu.eus
[2] Department of Electrical and Electronic Engineering, Auckland University of Technology, Auckland 1010, New Zealand; tek.lie@aut.ac.nz
[3] Jema Energy, Paseo del Circuito 10, CP 20160 Lasarte-Oria, Spain; jonander.lopez@jemaenergy.com
* Correspondence: aritza.camblong@ehu.eus; Tel.: +34-943-018-681

Abstract

Implementing an effective energy management system (EMS) is essential for optimizing electric vehicle (EV) charging stations (EVCSs), especially when combined with battery energy storage systems (BESSs). This study analyzes a real-world EVCS scenario and compares several EMS approaches, aiming to reduce operating costs while accounting for BESS degradation. Initially, significant savings were achieved by optimizing the EV charging schedule using genetic algorithms (GAs), even without storage. Next, different BESS-based EMSs, including rule-based and fuzzy logic systems, were optimized via GAs. Finally, in a dynamic scenario with variable electricity prices and demand, the adaptive GA-optimized fuzzy logic EMS was found to achieve the best performance, reducing annual operating costs by 15.6% compared to the baseline strategy derived from real fleet data.

Keywords: energy management systems; electric vehicle charging stations; lithium-ion batteries; rule-based algorithms; fuzzy logic; genetic algorithm

Received: 9 July 2025
Revised: 30 July 2025
Accepted: 30 July 2025
Published: 8 August 2025

Citation: Olano, J.; Camblong, H.; López-Ibarra, J.A.; Lie, T.T. Development of Energy Management Systems for Electric Vehicle Charging Stations Associated with Batteries: Application to a Real Case. *Appl. Sci.* **2025**, *15*, 8798. https://doi.org/10.3390/app15168798

1. Introduction

The transportation sector accounts for 23% [1] of the total greenhouse gas (GHG) emissions. Electric vehicles (EVs) have emerged as a promising solution to this issue. Among the different transport sectors, public transport plays an important role in the transition to a cleaner transport industry. In particular, the electrification of bus fleets is a significant issue, as buses are the most used public transport vehicles around the world [2].

The high charging power demand of EVs can produce large voltage fluctuations and instability in grid interconnection. Moreover, economic viability is a key factor in this transport electrification transition. In this context, the EMS of EV charging stations (EVCSs) has a noteworthy influence [3] on the prosperity of these systems. In addition, BESSs are a good solution to the aforementioned fluctuations, especially with respect to increasing the flexibility of an EMS. In this way, a BESS can not only make a system more robust but also reduce greenhouse gas emissions by 24% compared with conventional grid-based charging without an energy storage system (ESS) [4]. On the other hand, even though photovoltaic (PV) installation with a vehicle-to-grid (V2G) application can result in a 50% reduction in charging cost [5], there are many cases where the installation of renewable sources is not profitable or the installation of a V2G system is not allowed by the grid operator. In

that kind of scenario, ESS installation is still interesting. It is a central element for moving the charge of EVs over time and thus decreases the charging cost and damps the possible fluctuations, as mentioned before. Regarding the BESS converter's topology, in [6] it is concluded that a direct-current (DC) branch connection with the charging station and the BESS in parallel (Figure 1) is the best option if the aim of the ESS is to reduce the grid consumption without injecting power into the grid. Concerning the different options for ESSs, lithium-ion batteries are the best choice for energy-related applications where a high C-rate is not required [7].

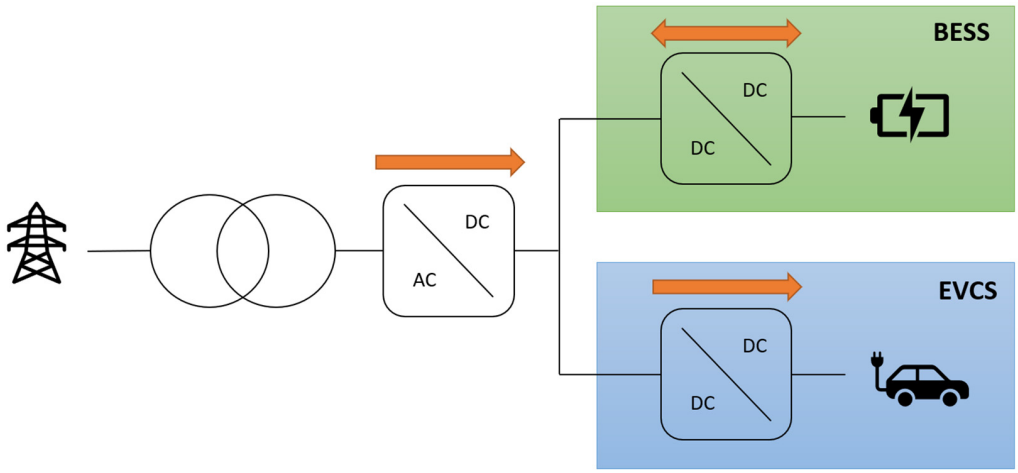

Figure 1. DC branch topology of a grid connected to an EVCS associated with a BESS in parallel. The orange arrows indicate in which direction the power can flow in each converter of the system. It can be seen that no power is injected into the grid and that the electric vehicles are used only for charging.

With regard to EMSs, many different strategies are proposed in the scientific literature, as illustrated in [8] for an application to hybrid EVs. When it comes to optimization strategies, diverse methods are used, such as the dynamic programming approach [9], grouping genetic algorithm (GGA), and Markov decision process [10]. As far as learning-based methods are concerned [11] (reinforcement learning, neural networks, and unsupervised learning), they are very costly at the computational level [12]. A proper EMS can lead to a considerable cost reduction in the system to which it is applied; in [13], the power distribution of a microgrid was optimized using multi-objective genetic algorithms (MOGAs), which resulted in a potential cost reduction of 16%.

Regarding EVCS charging schedule optimization, in [14], it was concluded that SOC-optimized managed charging can lead to a 13.5% reduction in the total charging costs of the charging station. In [15], a comprehensive analysis of a co-optimized microgrid with EVs was carried out, with the objective of applying a procrastination policy for charging the EVs. The results show that the policies can be easily implemented in real time and that they have a positive impact on cost reductions in the system. However, the need to carry out further research on a large-scale fleet, instead of a simple analysis of a single EV, is identified. In [9], the total cost of an EVCS was reduced by 50% by applying a combined approximate dynamic programming and evolution algorithm to determine the optimal charging time for each EV. For a large-scale EV charging scenario, a hybrid approach combining genetic algorithms (GAs) and dynamic programming is considered to be very effective in reducing the total cost of system operation [16]. More papers can be found on optimal charging scheduling from the grid [17–19].

As mentioned above, the integration of a storage system gives more flexibility to the EMS and thus can allow the economic optimization of microgrids or hybrid energy systems. In [20], energy cost minimization was carried out with respect to the design of an EMS for a

hybrid storage system operating in a microgrid with PV installation. The cited study shows how important it is for an EMS to consider a technoeconomic model of the microgrid in order to reduce microgrid costs. In addition, the authors show that charging the BESS with the entire surplus PV power is not economically profitable, as the battery degrades further, increasing the overall cost. In [21], the importance of optimally managing BESSs in order to lengthen their lifetimes and thus decrease their costs is also highlighted. In [22], an EVCS with PV and BESSs is analyzed. The aim was to economically optimize the BESSs by using a new rule-based (RB) strategy. The cited study considers a degradation cost model of the BESSs and the volatile price of the grid in the minimization of the overall EVCS cost. The authors conclude that implementing a proper EMS reduces the cost of the system and that the benefit of BESSs is greater when the electricity price has a large variance. In [23], a BESS and a hydrogen station were integrated into an EVCS, and different possible strategies were compared. The authors concluded that a 31.53% cost reduction could be achieved by optimizing this system.

Numerous articles have studied the optimal power flow of BESSs for cost reduction [3–9,14–22], but few studies have been found in which BESSs are not connected to a renewable energy source [6,7]. Moreover, many studies do not consider the degradation cost of BESSs [3–7,12], while other manuscripts highlight the importance of this cost when carrying out a cost optimization of a system containing a BESS [20–22]. Finally, in this context, the authors of this article have not found any methodology for developing an EMS that can easily adapt to different EV charging scenarios and electricity price fluctuations.

In this manuscript, a study on the development of technoeconomically optimized EMSs for EVCSs for a real-life case of an urban bus fleet associated with BESSs (as in Figure 1) is presented. This research focuses on an electric bus fleet charging station but can be adapted to any kind of EV fleet charging station that has a fixed available charging time for each electric vehicle. Regarding the literature, an optimized EMS design for variable loads and grid electricity prices has not been found. Moreover, grid electricity price-sensible adaptive EMSs have not been found either. It is also noticeable that the degradation cost of BESSs is not taken into account in many studies, while in others it is remarked to be an important factor when trying to optimize the utility of a BESS. Considering the existing knowledge gaps identified in the scientific literature analysis, the main contributions of the study are as follows:

- The comparison between a real charging strategy EMS and optimized ones.
- The consideration of the BESS degradation cost in an optimized EMS.
- The design and comparison of different RB and FL EMSs optimized with a GA, in realistic varying study cases.
- The design of an adaptive EMS depending on the forecasted electricity price.
- The use of an optimized FL EMS in a BESS integrated into an EVCS.

In the next section, the abovementioned methodology is described. Then, in the following section, this methodology is applied to a specific case study and the obtained results are analyzed and discussed. The last section gives the main conclusions of the research study.

2. Designed Methodology

The designed methodology is illustrated in Figure 2 and contains six steps divided into three main stages. The first stage does not consider a BESS in the system. At this stage, the main characteristics of the EVCS and the associated constraints are defined. In addition, optimization of the charging schedule of the buses is performed by using a GA, since this optimization technique is considered effective for this type of complex problem due to its stochastic approach [16]. For the second stage, a BESS is modelled and integrated into the

system. In this second stage, different EMSs with which to control the BESS are designed and optimized, using a GA to minimize the cost of operation of the system. In the third stage, a varying grid electricity price scenario is first defined. Based on the optimized EMS, an adaptive EMS is designed for the next-day price profile. Finally, all of the designed EMSs are evaluated in a wide scenario (varying price and load power profiles) to see which one has the best economic performance.

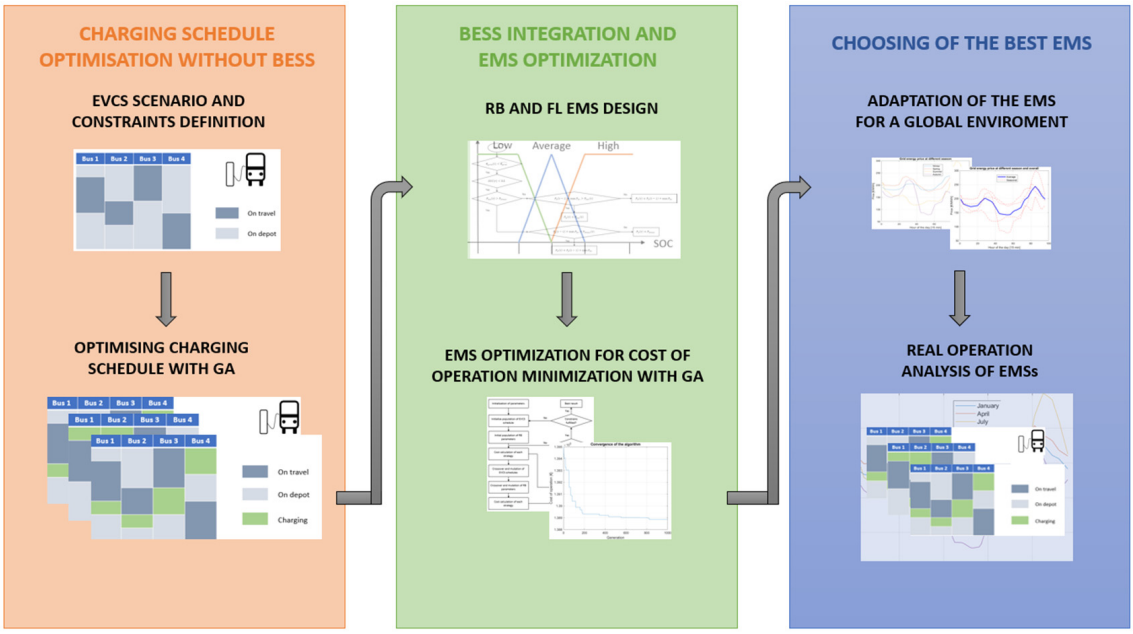

Figure 2. EVCS EMS design methodology.

2.1. Stage 1: Charging Schedule Optimization Without BESSs

2.1.1. EVCS Scenario and Constraint Definition

EVCSs are built by assembling the same number of chargers as the number of plug-in EVs. In order to define the load profile of the station, a 15-min-step profile is used, and the study is focused on an urban fleet of electric buses. The buses have a certain daily driving schedule, where the time they are on the move and in the depot is distinguished, as shown in the example of Figure 3. **The original charging strategy of the bus fleet can be seen in Figure A1, which is the original charging schedule of a public bus fleet**.

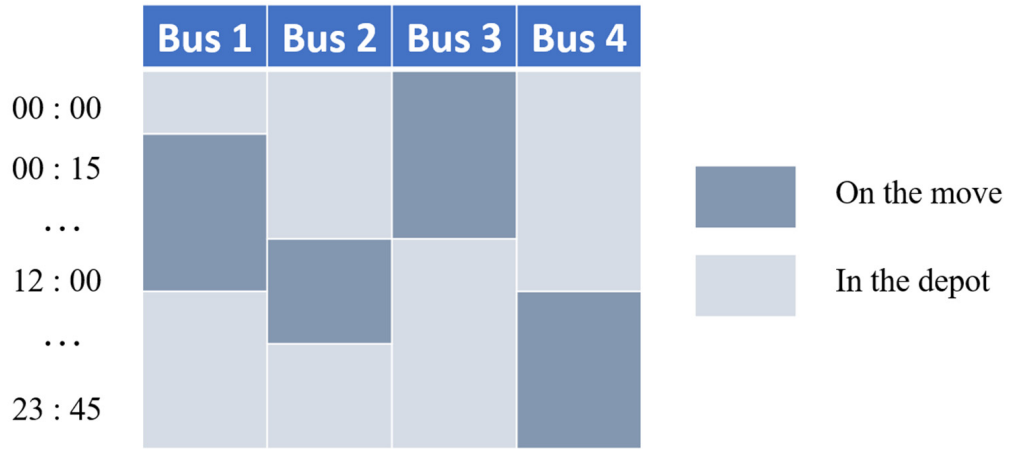

Figure 3. Basic illustration of the time during which buses are on the move and in the depot.

Three constrains are defined. The first one is related to the maximum power contracted from the grid:

$$P_{Gmax} \geq P_{EVCS}(\mathrm{t}) = \sum_{n=1}^{N} P_{EVCS}(\mathrm{n},\mathrm{t}) \quad (1)$$

$P_{EVCS}(t)$ is the total power required by the buses at each time step ($P_{EVCS}(\mathrm{n},\mathrm{t})$ for the nth charger) and N is the number of chargers.

Buses batteries must contain enough energy, $E_B(\mathrm{n})$, in order to be able to drive the whole route over the day:

$$E_B(\mathrm{n}) = \sum_{t=1}^{T} P_{EVCS}(\mathrm{n},\mathrm{t}) \quad (2)$$

In addition, the nth EV charger power, $P_{EVCS}(\mathrm{n},\mathrm{t})$, is limited to a maximum value:

$$P_{EVCS}(\mathrm{n},\mathrm{t}) \leq P_{Cmax} \quad (3)$$

2.1.2. Optimization of the Charging Schedule Using GA

The analyzed system has a wide range of search space; thus, a stochastic population-based evolutionary algorithm, such as a GA, fits much better than a stochastic individual-based algorithm. Among the group of evolutionary algorithms, GAs have some advantages: they are flexible, and the best individual of each iteration survives for the next population.

Each gene of the chromosomes of the GA represents a whole-day schedule of the bus fleet, where the time each bus is on the move and the time it is at the depot are defined. Therefore, the whole gene of a chromosome is a 96xN matrix that represents a possible charging scenario of the whole bus fleet.

Optimization Function

The objective of this first EMS, EMS1, is to minimize the charging cost of the EV fleet without considering BESSs. Thus, the function to be minimized, i.e., the fitness function of the GA, is as follows:

$$f = \sum_{n=1}^{N} \left(\sum_{t=1}^{T} P_{EVCS}(n,t) \cdot €_G(t) \cdot S_D(n,t) \cdot \eta_C^{-1} \right) \quad (4)$$

$€_G(t)$ is the grid electricity price at interval t, η_C represents the efficiency of the EVCS converters, and $\mathrm{S_D}(n,t)$ is a binary variable that defines if the nth bus is on the move ($S_D(n,t) = 0$) or at the depot ($S_D(n,t) = 1$).

GA Technique Selection

The different techniques used in each step are described in this section. A penalty function is applied to the fitness function calculation so that the chromosomes related to all cases where a constraint is not respected do not survive the next generation.

2.2. Initial Population

The first chromosome is created by using the original charging strategy, which is shown in Figure A1 The other chromosomes are created from this first chromosome by shifting the charging start time, always inside a feasible timetable.

2.3. Selection

First, the analyzed population is ranked depending on its fitness function, from best to worst. If a chromosome's fitness is outside of feasible values (because of the mentioned penalty), it is taken out of this ranking. Then, the normalized fitness value of each chromosome is calculated, and a cumulative value is given to each chromosome, where the best chromosome takes a value of 1 and the worst one takes its normalized value. Then, a random value between 0 and 1 is compared with this cumulative value, and the last chromosome with highest cumulative value compared to the random one is taken as

a parent for the next generation. Then, a random value is taken between 0.5 and 1 and another parent is chosen, so at least one of the parents is in the 50% of best chromosomes, increasing the exploitation.

2.4. Crossover

The used technique is an adaptation of crossover. At first, one number is chosen randomly between X possible numbers; in this work, three possibilities are defined: 0, 1, and 2. If 0 is chosen, a single-point crossover is performed; if 1, is chosen a 2-point crossover is performed; and, if 2 is chosen, a uniform crossover is performed. Any crossover is performed with a probability of 0.85. As many techniques are involved, an average value of the recommended crossover percentage from the literature has been taken.

2.5. Mutation

Two different mutations are performed, both with a probability of 1% for each gene: a full mutation where the charging of a bus is randomized, and a local mutation where the charging power is mutated.

For the full mutation, the whole charging schedule of a bus is changed. This new charging schedule is performed randomly with different powers (limited by the maximum power of the chargers) at any possible time that the bus is in the depot.

Regarding the local mutation, the power at the cheapest time inside that charging time range is increased, while the most expensive time power is lowered at the same rate.

The parameters used for the crossover probabilities (P_{cP} and P_{cSOC}) and mutation probabilities (P_{mP} and P_{mSOC}) are given in Table 1 [24].

Table 1. Evolution probability parameters for the charging schedule optimizer GA.

Parameter	Value
P_{cP}	0.85
P_{cSOC}	0.85
P_{mP}	0.01
P_{mSOC}	0.01

2.6. Elitism

Four chromosomes are chosen by elitism at the end of each iteration of the genetic algorithm. By performing this, the new population is at least as good as the one before, as the four best chromosomes with the best fitness are always preserved for the next generation.

2.7. GA Tuning

After a sensitivity analysis of GA parameter tuning, a population size of 90 chromosomes and a number of 5000 iterations have been chosen.

2.8. Stage 2: BESS Integration and EMS Optimization

2.8.1. BESS Integration and Modelling

According to the literature [4,7,21,22], installing a BESS is very useful for EVCS microgrid systems. The degradation of BESSs has an important influence on the total cost of the operation [20,21], and the BESS constraints have to be considered by the EMSs. Thus, the BESS is modelled in order to represent the mentioned constraints and degradation.

Electric Model

A battery is usually characterized by the open-circuit voltage of the battery pack, and the internal resistance of the battery pack. Using these parameters and knowing the power

of the BESS (given by the EMS), the current of the BESS, I_{BESS}, can be calculated as in Equation (5), taken from article [25]:

$$I_{BESS} = \frac{U_{BESS}(\text{SOC}) - \sqrt{U_{BESS}^2(\text{SOC}) - 4 \cdot P_{BESS} \cdot R_{BESS}(\text{SOC}) \cdot (-sign(P_{BESS}))}}{2 \cdot R_{BESS}(SOC)} \quad (5)$$

where U_{BESS} is the open-circuit voltage of the battery pack, R_{BESS} is the internal resistance of the battery pack, and P_{BESS} is the power output of the battery pack. Then, the battery SOC is obtained by using the coulomb counting method represented in Equation (6) [25]:

$$SOC_{BESS}(k) = SOC_{BESS}(k-1) - \frac{I_{BESS}(k-1) \cdot \Delta t}{C_{BESS0}} \quad (6)$$

where Δt is the time step of 15 min between the actual and previous states of charge, C_{BESS0} is the initial capacity of the battery in Ah, and k is the actual time step.

Degradation Model

Once the SOC data are obtained, the model described in [21] is used to calculate the BESS degradation cost. Only the degradation due to cycles is considered, without taking into account the calendar degradation. Indeed, even though the ageing mechanism of BESSs is complex, it is mainly related to the depth of discharge (DOD) and to the charge as well as discharge cycles. The higher the battery's DOD, the fewer cycles it will endure, and the greater the degradation of the battery [21]. This relation is represented by Equation (7):

$$N_{cycle} = \beta_0 \cdot DOD^{-\beta_1} \cdot e^{\beta_2 (1 - DoD)} \quad (7)$$

where N_{cycle} is the number of cycles of the BESS, and $\beta_0 = 1.05 \times 10^7$, $\beta_1 = 0.8159$, and $\beta_2 = 0.098$ are parameters that depend on the chemistry of the battery (values taken from the specific battery of the project).

The operation or degradation cost of the BESS depends on the number of cycles the battery performs with a given DOD and the total BESS capital cost. As $DOD = 1 - SOC$, from Equation (7), the operation cost can be defined as follows:

$$C_{BESSop}(SOC) = \frac{C_{BESScap}}{N_{cycle}} \quad (8)$$

where $C_{BESScap}$ is the total capital cost of the BESS and C_{BESSop} is the operation or degradation cost of the BESS.

This equation is valid only if two assumptions are taken into account: (i) the charge and discharge operation for a given DOD has a uniform impact on cell degradation and (ii) the charge or discharge cycle is independent of the previous cycles.

In order to relate the partial charge/discharge cycles of the BESS, the rainflow-counting algorithm is used [21]. This method considers all of the partial charge/discharge profiles and relates them to some charge/discharge cycles that start from full capacity until the minimum SOC reached on the respective partial charge/discharge. Therefore, the cost of the partial charge/discharge is calculated as illustrated in Figure 4 (taken from [21]), and the total BESS operation cost is the sum of each cycle cost.

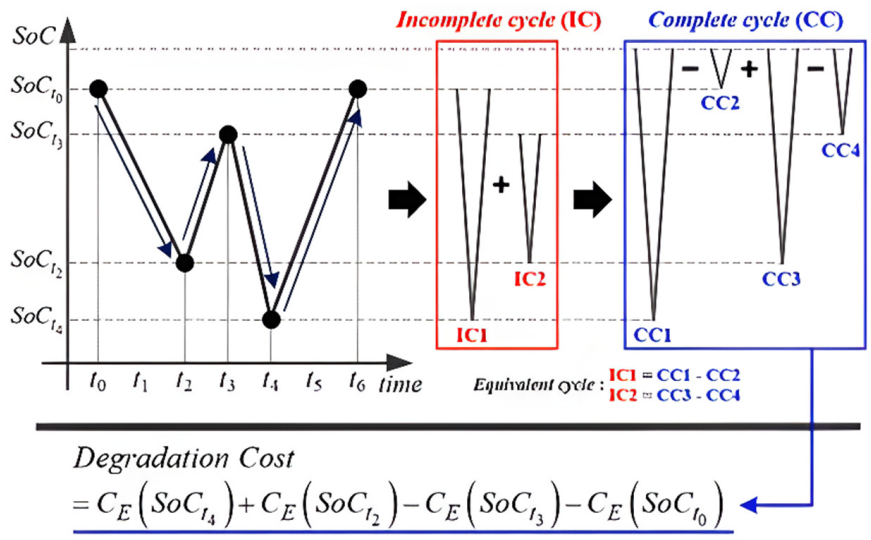

Figure 4. Operation/degradation cost calculation based on the rainflow-counting method [21].

Thus, the total degradation cost is calculated as follows, adding the degradation related to each partial cycle and relating it to a full cycle:

$$C_{BESSop}(SOC) = \sum_{t=1}^{T} C_E(SOC_t) \quad (9)$$

where C_E is the partial cycles of the BESS.

Constraints

Four constraints related to the BESS are considered:

A. The battery SOC, SOC_{BESS}, has to be between the minimum, $SOC_{BESSmin}$, and maximum, $SOC_{BESSmax}$, values provided by the manufacturer:

$$SOC_{BESSmin} \leq SOC_{BESS}(t) \leq SOC_{BESSmax} \quad (10)$$

B. The power consumed (considered as positive power) by the EVCS, P_{EVCS}, and the BESS, P_{BESS}, cannot be greater than the contracted power, P_{Gmax}:

$$P_{BESS}(t) + P_{EVCS}(t) \leq P_{Gmax} \quad (11)$$

C. The maximum power variation in the BESS in one sample interval is limited to $P_{BESSstep\_max}$:

$$|P_{BESS}(t) - P_{BESS}(t-1)| \leq P_{BESSstep\_max} \quad (12)$$

D. The BESS power does not have to exceed a limit, $P_{BESSmax}$:

$$|P_{BESS}(t)| \leq P_{BESSmax} \quad (13)$$

2.8.2. Design of a Non-Optimal EMS

The objective of the EMS is to charge the fleet bus batteries at the lowest possible cost. This cost depends on the grid tariff, which varies during the day, and on the BESS degradation/operating cost. The EVCS power schedule is that optimized in Section 2.1.2.

The input variables of the EMSs are the grid tariff, $€_G(t)$, the fleet load, $P_{EVCS}(t)$, and the SOC of the BESS, $SOC_{BESS}(t)$, while the output is the BESS power, $P_{BESS}(t)$. Two types of EMSs are designed, an RB (EMS2) and an FL (EMS3), the latter of which is better at considering uncertainties.

RB EMS

As shown in the flowchart in Figure 5, the RB EMS compares the grid power price with a threshold, $€_{Gthr}$, in order to decide whether to charge or discharge (A branch) the BESS. If the price is low, the BESS is charged. Depending on the SOC, charging is either fast (for SOC < 0.5) or slow (P_{BESS} and $P_{BESSstep\_max}$ at half their value, to avoid high DODs). This is rule is applied in order to reduce the degradation of the battery [21], and, thus, the cost of operation. Then, if $P_{diff}(t)$, the difference between the contracted maximum power, P_{Gmax}, and the fleet load at t sample interval, $P_{EVCS}(t)$, is higher than $P_{BESSmax}$, the maximum possible value is given to P_{BESS}.

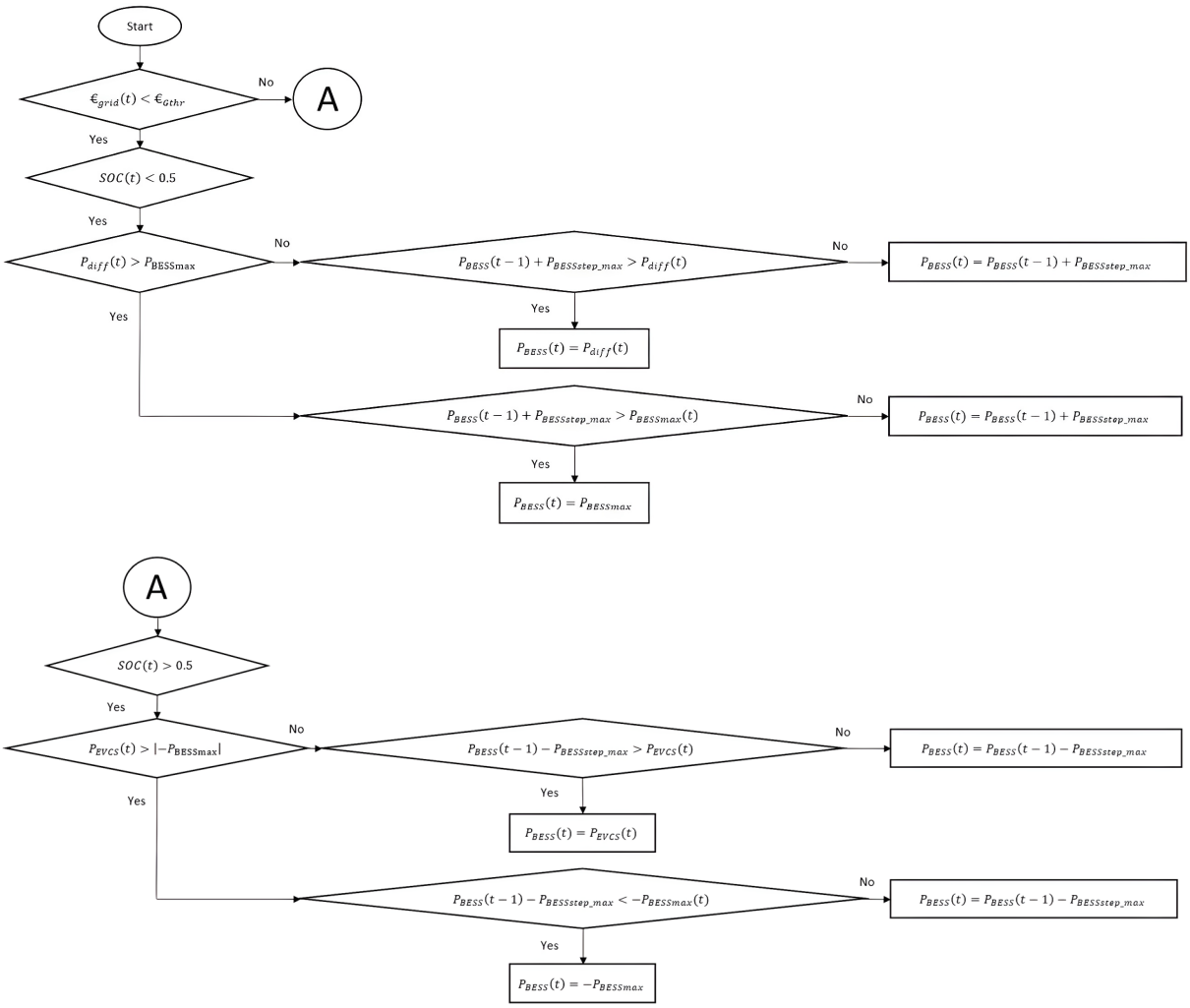

Figure 5. Logical flowchart of the RB EMS strategy.

The A branch follows the same logical structure but discharging the BESS, and, instead of using P_{diff} as the power limit, the available power to load the fleet is considered.

FL EMS

The RB EMS can be useful for simple management, but for complex problems, other EMSs are more suitable. RB EMSs have staggered output values, while for the control of battery power, a continuous value is more suitable. In this regard, an FL EMS was designed. It generates intermediate values between true and false, enabling the EMS to effectively manage inaccurate inputs. In this case, the three inputs have continuous values over time (electricity price, SOC, and demand power). Moreover, the output of the controller is

calculated as the weighted averages of multiple rules, which results in smooth transitions and control actions, reducing abrupt changes [26].

The design of the FL EMS has been carried out following the classical methodology [26]. The fuzzy sets are naturally the inputs and output of the EMS. In the definition of the linguistic variables, a balance has been achieved between the required precision for the variables in question and an acceptable amount of fuzzy rule. Therefore, the linguistic variables of the EMS inputs and output have been defined as follows:

- P_{BESS}: *CH* (fast charge), *ch* (slow charge), *0* (no charge/discharge), *dis* (slow discharge), and *DIS* (fast discharge).
- $€_{grid}$: *VH*, *H*, *L*, and *VL*.
- *SOC*: *VH* (very high), *H* (high), *AV* (average), *L* (low), and *VL* (very low).
- P_{EVCS}: *VH*, *H*, *AV*, *L*, and *VL*.

2.8.3. Optimization of the RB and FL EMSs

In this section, some parameters of the RB and FL EMSs are optimized in order to perform better. The optimization of the EVCS charging schedule and the BESS charging/discharging management parameters is performed in parallel.

Optimization Function

In order to minimize the cost of the entire charging system, two criteria are considered: the grid price at which energy is charged in the buses and the BESS degradation cost, $C_{BESSdeg}$:

$$f = \sum_{n=1}^{N} \left(\sum_{t=1}^{T} P_{EVCS}(n,t) \cdot €_G(t) \cdot S_D(n,t) \cdot \eta_C^{-1} \right) + C_{BESSop} \quad (14)$$

The optimization processes presented in the following sections are carried out with the GA.

RB EMS Optimization

As mentioned in [8], the tuning of RB EMS parameters has a significant impact on results, especially when the rules are simple. Here, five parameters of the RB EMS are optimized: $P_{BESSmax}$, $P_{BESSstep\_max}$, $SOC_{BESSmin}$, $SOC_{BESSmax}$, and $€_{Gthr}$. Indeed, the maximum and minimum values of the SOC and P_{BESS} can be adjusted inside some limits imposed in the BESS data sheet. The genetic evolution of the power parameters is carried out as a block, as $P_{BESSstep\_max}$ is limited by $P_{BESSmax}$.

The GA that looks for the optimization of the abovementioned parameters is processed in parallel with the GA that optimizes the charging schedule of the buses (Figure 6). Thus, each charging schedule has one specific RB EMS, and the best individuals linked to the last schedule and RB EMS survive to the next generation.

Regarding the initialization, an array of fixed values on feasible range is defined. The maximum BESS power limits are defined between a very low power value of 30 kW (better regarding the degradation of the BESS [27]) to 2560 kW. Then, the maximum power step limits are defined between a low power value of 30 kW and a random value lower than or equal to the maximum power defined before. Regarding the maximum and minimum SOC values, they have to be between 0.7 and 0.95, and 0.3 and 0.05, respectively. Finally, the threshold price limits are between 0.16 and 0.22 EUR/kWh, near the average price value.

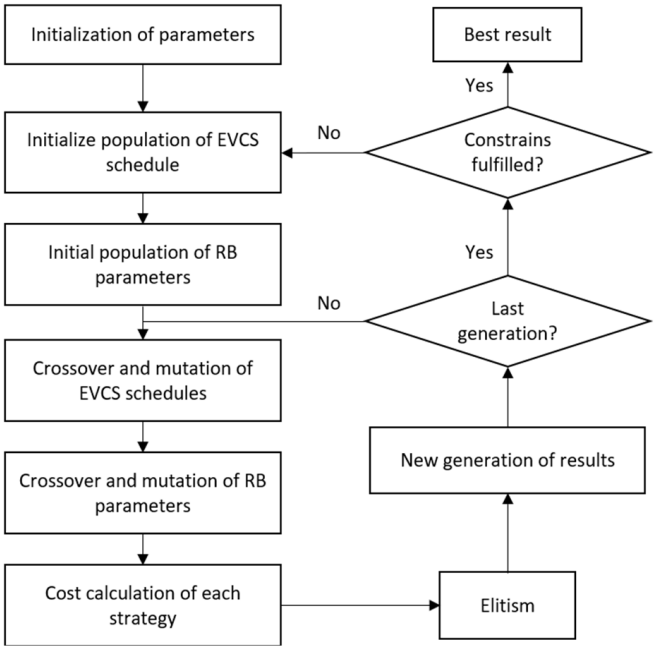

Figure 6. EVCS load and RB strategy optimization using GAs.

Concerning the crossover step, two crossover probabilities are calculated, one for the power parameters and another one for the *SOC* and $€_{Gthr}$ parameters. Then, two random values are computed and compared with the respective probability. If the random value is lower than the probability number, the crossover is performed. The crossover technique used is the same one as for the charging schedule, where a technique between single, double, and uniform crossover is selected randomly at each iteration.

Regarding the mutation, as in the crossover, a random value is computed for each group of parameters and, depending on if they are bigger than the fixed probability of mutating for each parameter, the mutation is performed individually on each parameter. The mutation of the parameters is carried out by randomly choosing a value within feasible limits, as in the initialization process.

Once all the steps are performed, a new population is created with X chromosomes and an RB EMS for each one. Then, the best individuals are selected from the last and current population to survive for the next generation. The process is repeated a fixed number of times (generations). At the end, the best combination of charging schedule and RB parameters is chosen. The parameters used for the crossover probabilities (P_{cP} and P_{cSOC}) and mutation probabilities (P_{mP} and P_{mSOC}) are those given previously in Table 1 [24].

FL EMS Optimization

Regarding the genetic optimization of the FL EMS, only the optimization of the membership functions (MFs) of the four fuzzy sets defined in Section 2.8.2 have been considered. The MFs in the corners have been defined as trapezoidal, and the others as triangular (Figure 7). Thus, 49 parameters are considered in the GA. Compared with the RB approach, a value in the X-axis can be in the range of *VL* to *L*. This is why the FL EMSs are useful for applications in uncertain regions.

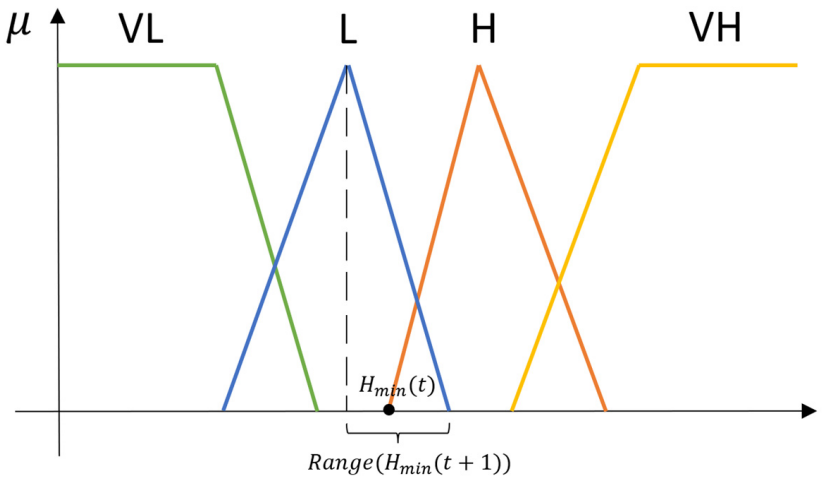

Figure 7. MF example. μ is the weight value (between 0 and 1), the green line represents the values that the "Very Low" (VL) MF takes when the variable in the X-axis is in that range, and the blue, orange, and yellow lines represent the "Low" (L), "High" (H), and "Very High" (VH) MF values, respectively.

The crossover operation has been performed by considering each linguistic variable in a same block, using three techniques randomly, the single, the double, and the uniform crossover.

Each parameter is mutated with a certain probability value, inside a feasible range, as shown in Figure 7 for the H MF minimum value (H_{min}). The mutation logic is a non-uniform mutation described in [28]. It has a large effect at the first iterations but no effect at the end. Each point of the MF is moved randomly in its possibility range as before, but now the change is multiplied by a decreasing factor over each new generation ($(1 - g/G)^b$). Therefore, each mutated parameter, $v\prime$, is defined by Equations (15) and (16) with the same probability:

$$v\prime = v + (v_{max} - v) \cdot r \cdot \left(1 - \frac{g}{G}\right)^b \quad (15)$$

$$v' = v - (v - v_{min}) \cdot r \cdot \left(1 - \frac{g}{G}\right)^b \quad (16)$$

where v is the last value of the parameter before being mutated, g is the current generation, G is the maximum generation, $b = 2$ is the parameter that defines the non-uniformity level, $[v_{min}, v_{max}]$ is the range of the parameter, and r is a random value between [0, 1]. It has to be noted that the bigger the maximum generation limit, the more exploitation is performed.

2.9. Stage 3: Choosing the Best EMS

2.9.1. Adaptation of the EMS for a Global Environment

In the previous section, optimization was carried with one day of data. As a next step, to generalize, the optimization of the FL controller is performed with grid price data of a representative whole month. This testing month is described in Section 3. In addition, the optimized FL EMS can be improved by considering an adaptive approach, by taking into account the variation in the day grid price profile. For that, a relationship is established between the optimized parameters of the FL EMS price MF and the grid price profile.

2.9.2. Comparison of the EMSs

Once the EMSs are designed, all of them are evaluated under the same scenarios that consider 30 different EVCS power demand profiles and 4 different grid price day profiles.

The cost of operation of the EMSs is compared for each possible case, and the one with the lowest economic cost is chosen as the best option.

3. Development of the EMS and Obtained Results for a Specific Case Study

The development of the methodology described in the previous section depends on the results obtained through some other steps. This is why its development and the results are presented and discussed in the same chapter.

3.1. Specific Case Study

The case study is an EVCS that charges an urban fleet of 89 electric buses at a sampling interval of 15 min. There are as many chargers as buses. The case and associated bus drop-off times are taken from a real-life example. **The original charging schedule can be seen in Figure A1.**

The maximum power contracted from the grid, $P_{G_{max}}$, is limited to 2 MW. The energy that each bus requires for a day, $E_B(n)$, is 960 or 1380 kWh, depending on the bus route. The maximum power that a charger can provide, $P_{C_{max}}$, is limited to 120 kW. This value is consistent with fast DC charging [29]. Regarding the grid tariffs, four specific daily price profiles are taken from the OMIE webpage [30], with the aim of representing the variability in grid tariffs over a year.

3.2. Optimization of the Charging Schedule Using a GA

A sensitivity analysis of the effect of the number of generations and chromosomes on the cost and the processing time has been performed. A compromise between the cost and the time has led to 1000 generations and 90 chromosomes. With these parameters, 10 optimization processes that lead to slightly different results have been carried out. Figure 8 shows the best day charging profile obtained. The blue curve represents the power required from the buses while the red one is related to the grid electricity price. When this price is high, the power demanded decreases, and the inverse is also true.

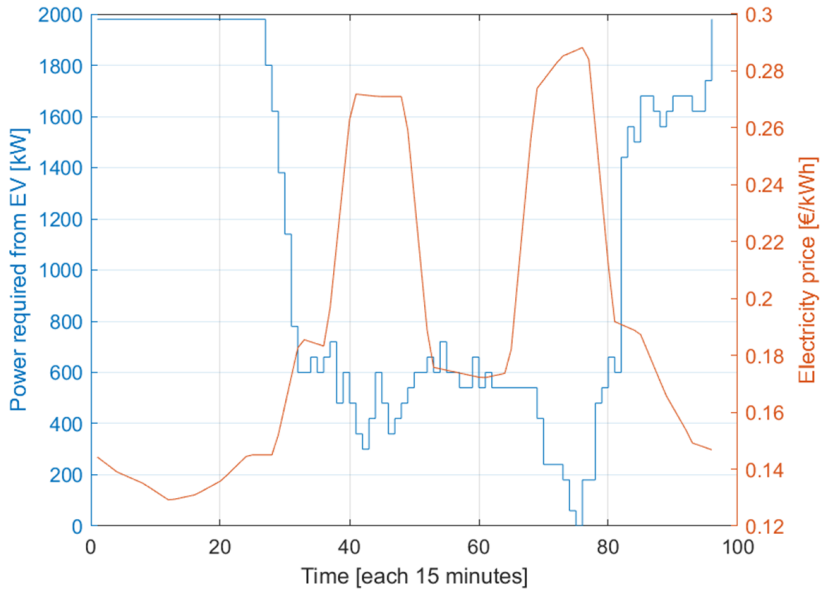

Figure 8. EVCS optimized charging profile. The left y-axis is used for the blue line, which refers to the EVCS power consumption, and the right y-axis is used for the red line, which refers to the electricity price at each moment.

The optimized charging profile performs 10% better than the original charging schedule, which can be seen in Figure A1.

3.3. BESS Characteristics

The capacity of the BESS is 2560 kWh. The values of the BESS open-circuit voltage and resistance are $U_{BESSoc} = 1500$ V and $R_{BESS} = 0.05\ \Omega$. As the system is an energy-oriented application, the output power that the battery can provide is capped to $P_{BESSmax} = 2560$ kW. The maximum power change in one sample step is $P_{stepMAX} = 100$ kW. With regard to the capacity limits, the minimum SOC is set to $SOC_{BESSmin} = 5\%$ and the maximum to $SOC_{BESSmax} = 95\%$. These limits are very usual for standard li-ion batteries.

As mentioned, SOC and P_{BESS} minimum and maximum values can be modified in the frame of the optimization processes, while they respect the data sheet limits. The values given above are initial values.

For the chosen size of the battery, the open-circuit voltage, $U_{B_{oc\_v}}$, is 1500 V, and the internal resistance, R_B, is 0.05 Ω. For the degradation cost calculation of the BESS, an inversion of $C_{cap} = 600$ k€ is supposed, as proposed in [31] for a BESS of this size.

3.4. Non-Optimal EMS

3.4.1. RB EMS

Once the BESS is characterized, the RB algorithm described in Section 2.8.2 has been used in parallel with the EVCS profile optimized in Section 3.2 in order to act on the BESS power. To understand the influence of the BESS on the new EMS, Figure 9 shows the obtained curves related to the EVCS power demand, in blue, and the grid power, in green, with the used price profile. They are similar to those of Figure 8, but the influence of the BESS integration is visible. When $€_G$ is high, P_{EVCS} is greater than P_G, i.e., the BESS contributes to bus charging. Inversely, the BESS is charged when $€_G$ is low. This behaviour is confirmed by the curves in Figure 10.

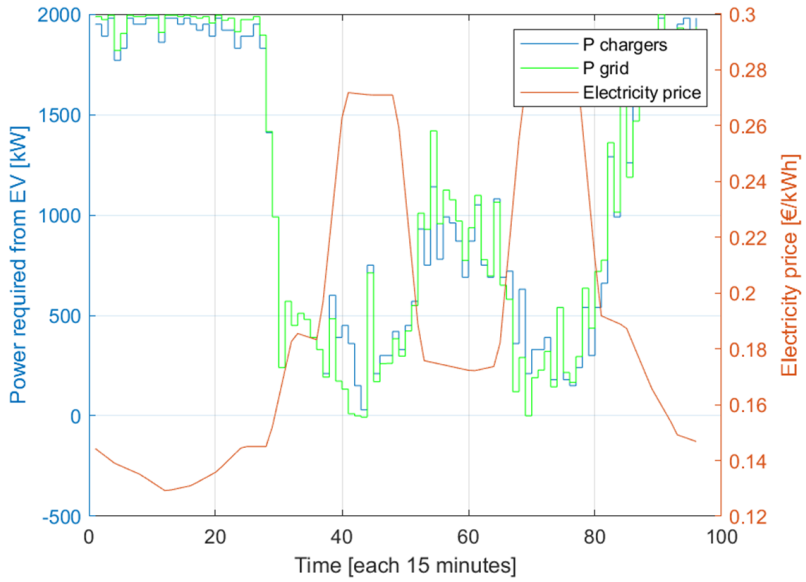

Figure 9. EVCS and grid power profiles obtained with the RB EMS. The left y-axis is used for the blue and green lines, which refer to the EVCS power consumption and the consumption from the grid, respectively, and the right y-axis is used for the red line, which refers to the electricity price at each moment.

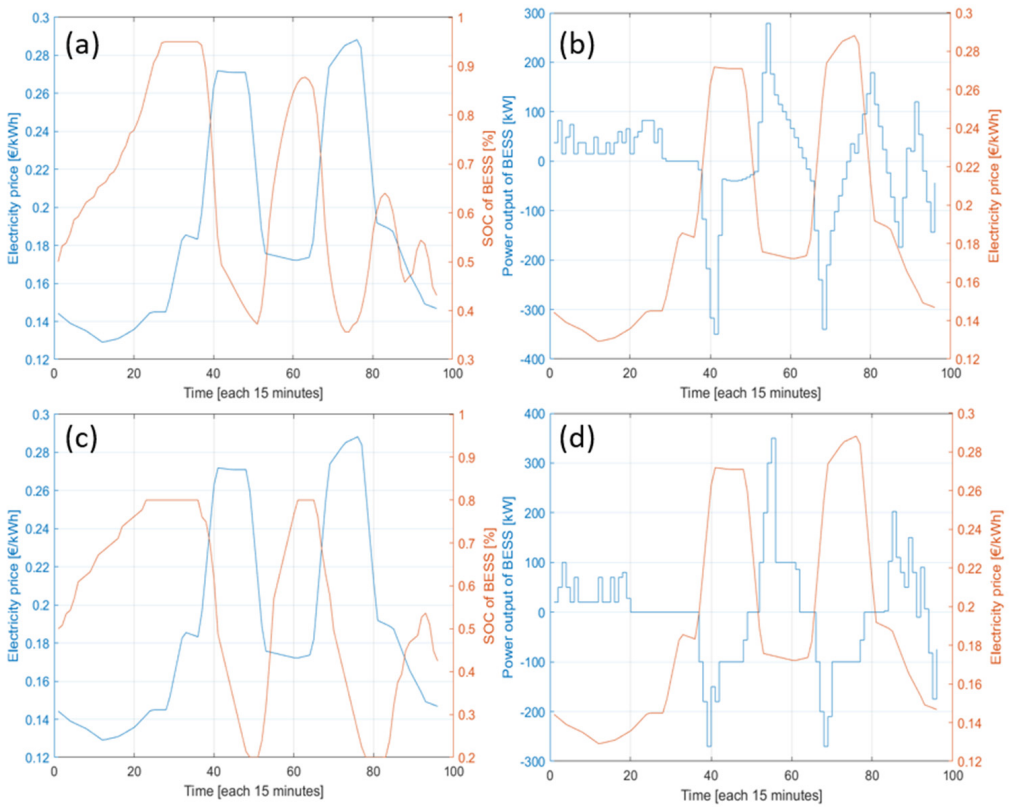

Figure 10. RB EMS response for a day. (**a**) BESS *SOC* during the day according to the electricity price for a *DOD* of 90%; (**b**) BESS power according to the electricity price for a *DOD* of 90%; (**c**) BESS *SOC* during the day according to the electricity price for a *DOD* of 60%; and (**d**) BESS power according to the electricity price for a *DOD* of 60%.

In addition, to study the influence of the *DOD* on the operation cost, it has been reduced from 90 to 60%, so that the BESS is operating at 80 to 20% of its capacity. The *SOC* evolution of the case can be seen in Figure 10's left windows, where in the lower window the maximum and minimum *SOC* are 0.8 and 0.2, respectively.

Compared to the original charging, the operation cost is reduced by 13% with the RB EMS and a *DOD* of 90%, and by 13.6% when the *DOD* is 60%. The degradation of the BESS is related to the *DOD*. Thus, even if with a reduced *DOD* the available power is lower, it can be interesting from an economical point of view.

3.4.2. FL EMS

Figure 11 shows the designed MF system for the four fuzzy sets.

Concerning the design of the FL EMS rules, decisions have been made following human reasoning. The rules are shown in Figure 12. The defuzzification has been performed with the Mamdani approach.

The BESS power and *SOC* evolution are similar to those shown in Figures 9 and 10. The operation cost obtained with this FL EMS is 12.7% lower than that of the original charging, i.e., a bit worse than with the RB EMS.

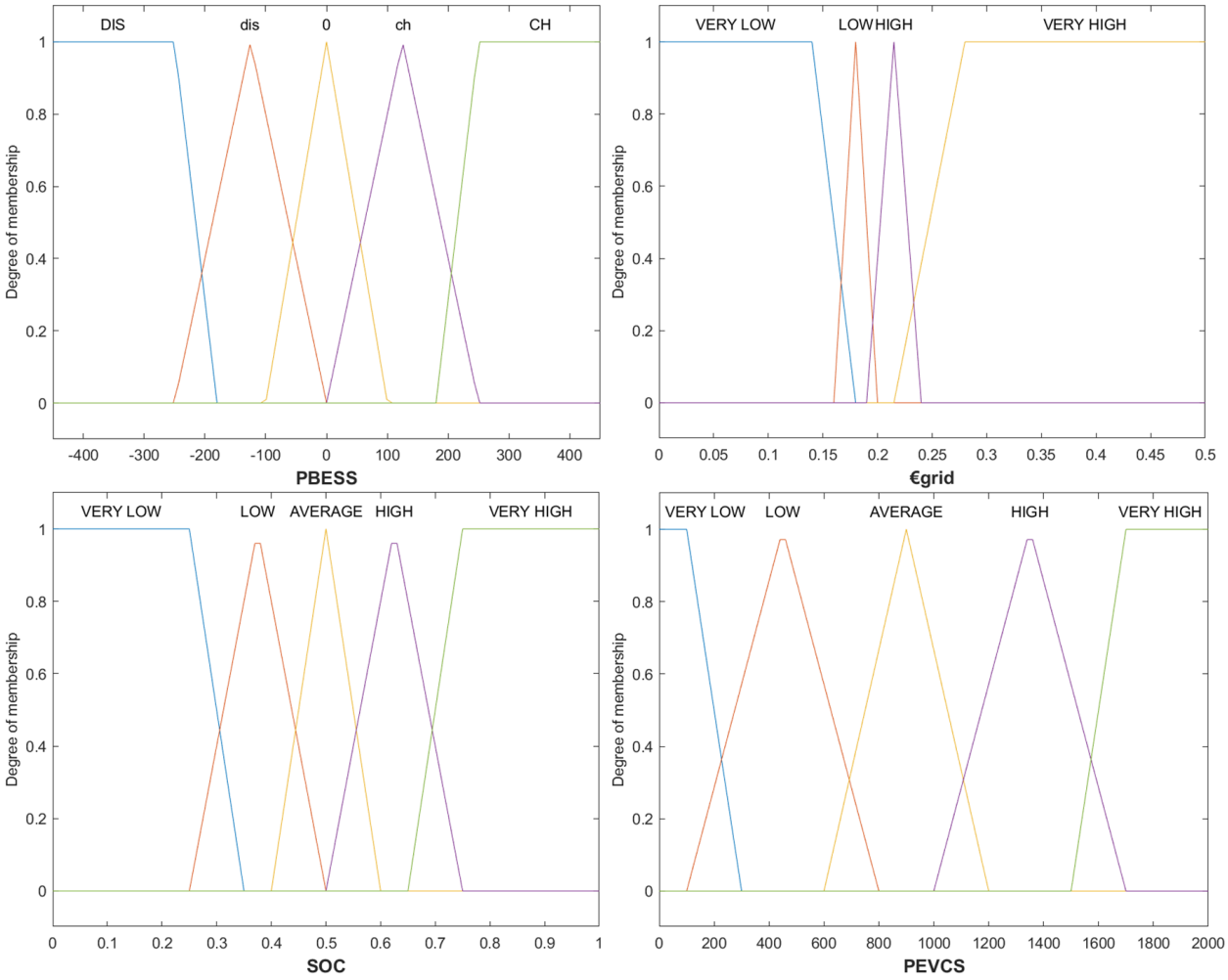

Figure 11. MF system for the four fuzzy sets.

***SOC* VH**		$€_{grid}$			
		VL	L	H	VH
P_{EVCS}	VH	dis	dis	DIS	DIS
	H	dis	dis	DIS	DIS
	AV	0	0	DIS	DIS
	L	0	0	DIS	DIS
	VL	0	0	DIS	DIS

***SOC* H**		$€_{grid}$			
		VL	L	H	VH
P_{EVCS}	VH	dis	dis	DIS	DIS
	H	0	dis	DIS	DIS
	AV	ch	0	DIS	DIS
	L	ch	0	dis	DIS
	VL	ch	ch	dis	DIS

***SOC* AV**		$€_{grid}$			
		VL	L	H	VH
P_{EVCS}	VH	0	0	DIS	DIS
	H	ch	0	DIS	DIS
	AV	ch	0	dis	DIS
	L	ch	ch	dis	dis
	VL	CH	ch	dis	dis

***SOC* L**		$€_{grid}$			
		VL	L	H	VH
P_{EVCS}	VH	0	0	dis	dis
	H	ch	0	dis	dis
	AV	ch	ch	0	0
	L	CH	ch	0	0
	VL	CH	CH	0	0

***SOC* VL**		$€_{grid}$			
		VL	L	H	VH
P_{EVCS}	VH	0	0	0	0
	H	ch	0	0	0
	AV	ch	ch	0	0
	L	CH	CH	0	0
	VL	CH	CH	ch	0

Input - SOC
Input - $€_{grid}$
Input - P_{EVCS}
Output - P_{BESS}

Figure 12. Defined fuzzy rules.

3.5. Optimization of the RB and FL EMSs

3.5.1. RB EMS Optimization

Ten optimization processes of the RB EMS have been computed using 90 chromosomes and 10,000 iterations. The obtained optimized parameters values for the best case were as follows: $P_{BESSmax}$ = 150 kW, $P_{BESSstep\_max}$ = 20 kW, $SOC_{BESSmin}$ = 35%, $SOC_{BESSmax}$ = 85%, and €$_{Gthr}$= 0.2 €. Regarding the obtained best operational cost, it is 14.3% better than that of the original charging.

3.5.2. FL EMS Optimization

The optimization of the FL EMS has been carried out as explained in Section 2.8.3. For the GA optimization, 90 chromosomes and 250 maximum generations have been used. The operation cost with this EMS is 15.4% better than in the original case. With fewer generations than in the other methods, the operational cost of the EV charging is lower.

3.6. Generalization and Adaptive Approach Applied to the FL EMS

Table 2 summarizes the EMSs that have been developed and the overall cost of operation obtained by each of them in one day of operation.

Table 2. EMS comparison according to their overall operation cost.

EMS	BESS	Optimized	Operational Cost [pu]
EMS0, original charging strategy	No	No	1
EMS1, optimized charging profile	No	Yes	0.9
EMS2, RB (90% *DoD*)	Yes	No	0.87
EMS2_b, RB (60% *DoD*)	Yes	No	0.864
EMS3, FL	Yes	No	0.873
EMS4, GA-RB	Yes	Yes	0.857
EMS5, GA-FL	Yes	Yes	0.846

These EMSs have been developed for a specific day grid price profile. Therefore, the good behaviour of these EMSs during a longer period with different price profiles and bus depot timetables is not ensured.

3.6.1. Generalization of the Optimized FL EMS

In order to enrich price profiles considering the different periods of the year, one profile has been created for each season of the year, based on OMIE data [30]. For each season of 2022, the month with the closest price value to the average of the season has been selected. To choose a representative day, the same strategy has been performed. Thus, 14 January, 14 April, 10 July, and 10 October have been selected. The price profiles of these days can be seen in Figure 13.

In addition to the grid price profiles, the different EV charging schedules that consider diverse bus timetables at the depot have been defined. Therefore, 20 different profiles have been created with an algorithm that charges buses randomly with varying demand power. In addition, the possible delay in the arrival of the buses at the depot has been considered, increasing the scheduled off-depot time with a certain probability. Moreover, the ten charging profiles obtained in the abovementioned RB EMS optimization process in Section 3.5.1 have been considered too, leading to 30 different charging schedules, one for each day of a month.

A new EMS, EMS6, is developed in this context, optimizing the FL EMS with 90 chromosomes and 1000 iterations, and applying the same constraints explained in Section 2.8.1. Figure 14 shows the obtained optimal MF systems. It can be seen that the forms differ from what would be a homogeneous distribution of the MFs (Figure 11).

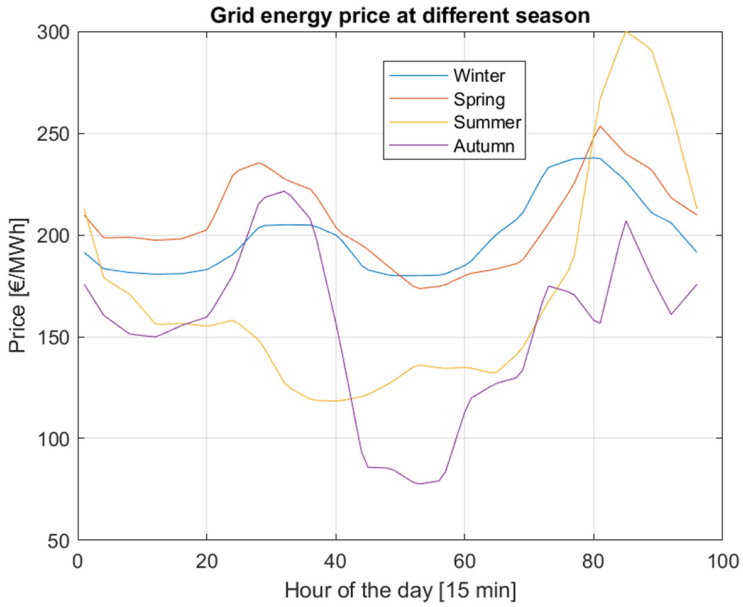

Figure 13. Seasonally representative profiles of the electricity price.

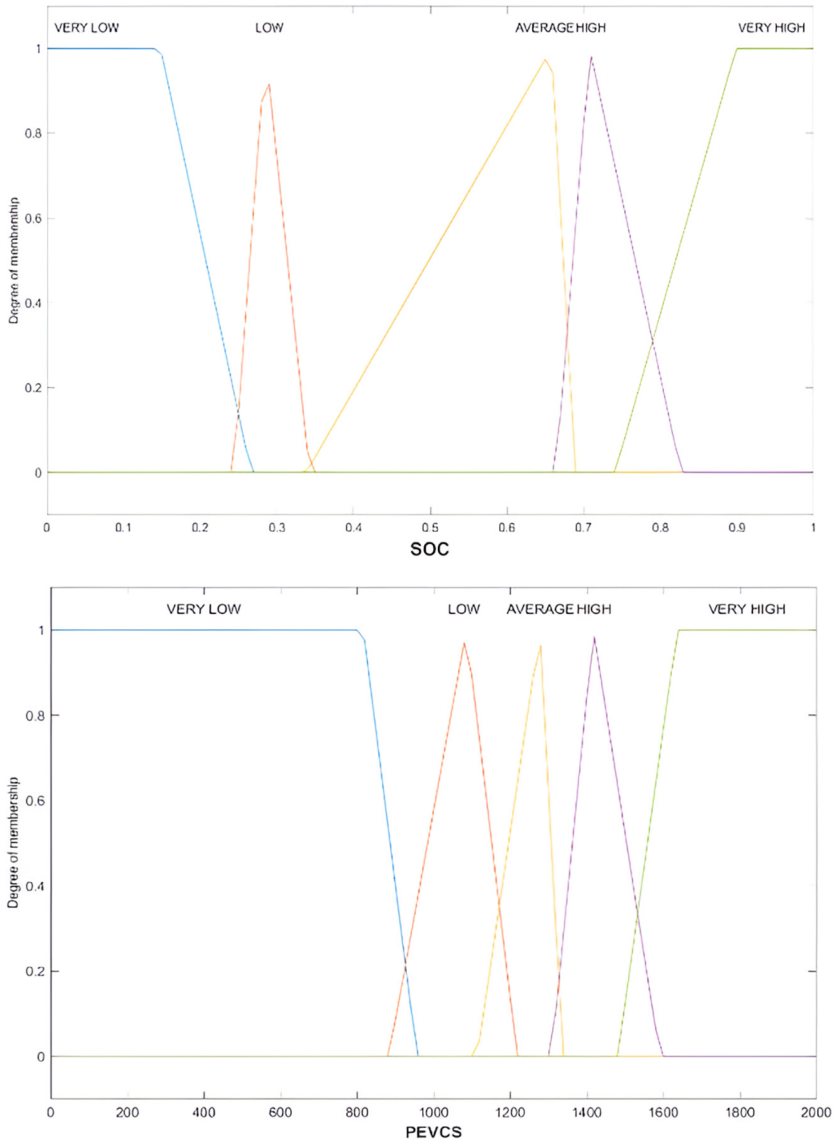

Figure 14. *Cont.*

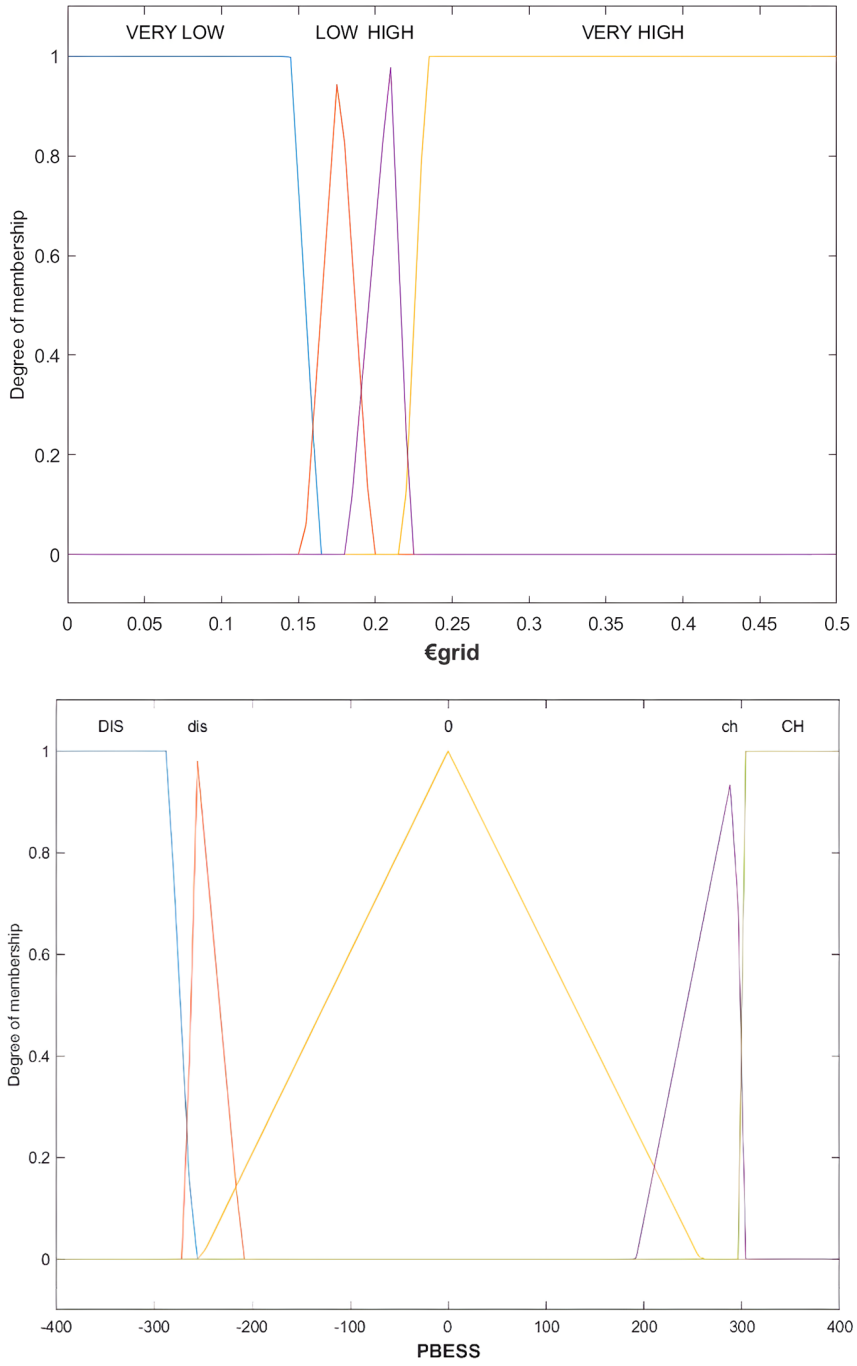

Figure 14. Optimized MF systems.

The obtained BESS output power behaviour for the month is shown in Figure 15, along with the electricity price profile. It can clearly be seen that the price changes have a direct effect on the behaviour of the BESS. Considering this influence, an adaptive FL EMS based on a one-day-ahead available forecasted price profile was designed, as explained in the next section.

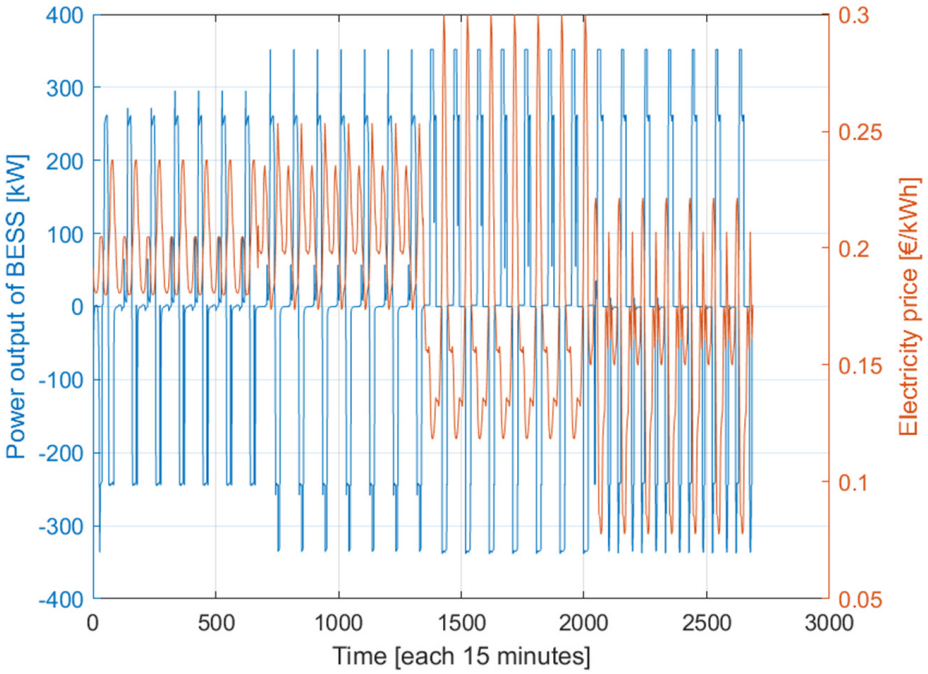

Figure 15. BESS output power and electricity power profiles for the month scenario.

3.6.2. Adaptive Approach of the Optimized FL EMS by Electricity Price Forecast

In order to adapt the MFs to the day-ahead price profile, an average price profile is calculated from the seasonal profiles (Figure 16), and a relationship is inferred between that profile and the optimized FL price MFs, as explained below. In Figure 16, the average price profile is shown with the optimized FL MF top values.

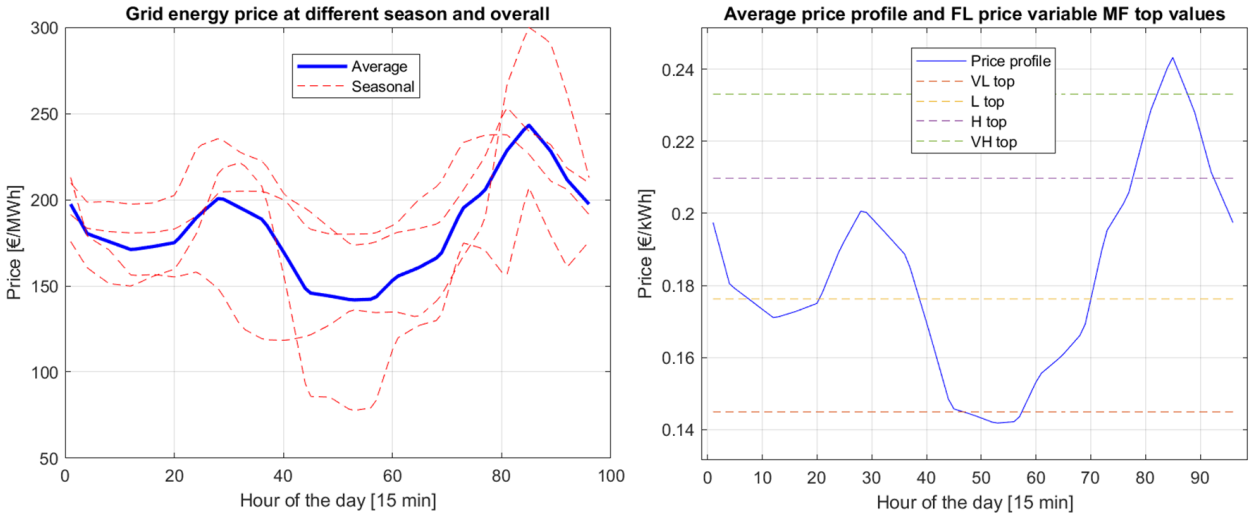

Figure 16. Annual average profile of the electricity price and FL EMS price MF top values.

A clear relation between the MF top values and the average price profile can be seen, and so the MF top values are defined as the next equations in the adaptative EMS:

$$VL_{top} = p_{min} + 0.05 \cdot (p_{max} - p_{min}) \tag{17}$$

$$VH_{top} = p_{min} + 0.95 \cdot (p_{max} - p_{min}) \tag{18}$$

$$L_{top} = p_{min} + \frac{(p_{max} - p_{min})}{3} \tag{19}$$

$$H_{top} = p_{min} + \frac{2 \cdot (p_{max} - p_{min})}{3} \quad (20)$$

The top values are almost proportionally distributed in the range from the minimum, p_{min}, to the maximum, p_{max}, price of the day. It should be noted that the limiting top values (VL and VH) are not on the maximum and minimum values of the price profile.

Regarding the maximum and minimum values of the MFs, they are fixed to have the same value as the top value of their adjacent MFs; in the optimized FL EMS, it can be seen that the values do not differ much from this logic (Figure 14). Moreover, now that the price MF system has been fixed, the top value of the 'average' *SOC* linguistic variable is fixed to 0.5, so that the BESS maintains its *SOC* near this value. This was not viable on the optimization of the EMS6, because only one price MF system was used for the whole scenario.

Using this price forecasting logic, two FL types have been designed—a Mamdani FL and a Sugeno FL—in order to analyze what could lead to better results.

3.7. Comparison of EMSs

A varying scenario has been created to know which EMS is the best for this case study. Some EMSs have been optimized for specific conditions, but this does not mean that they are the best ones overall, considering the 4 different price profiles and the 30 power load profiles. The 120 possible combinations have been simulated for 5 days to compare the best three EMSs: the optimized GA-FL (EMS5), the adaptive Mamdani-type FL (Ad_Mandani_FL), and the adaptive Sugeno-type FL (Ad_Sugeno_FL).

Figure 17 shows in what percentage of the 120 cases each EMS is the best option.

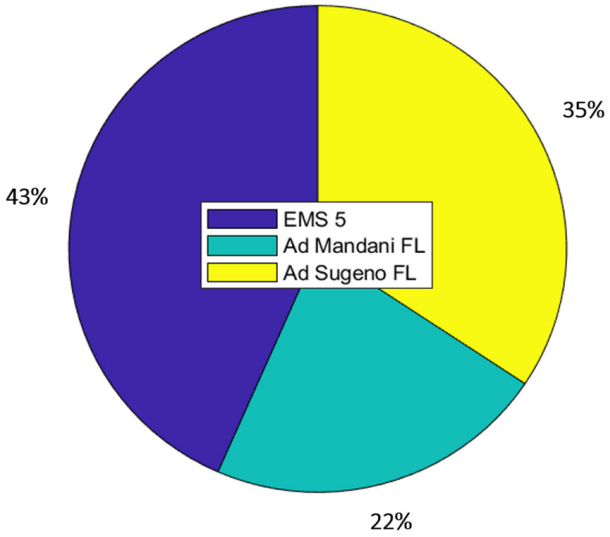

Figure 17. Percentage of optimized GA-FL (EMS5), the adaptive Mamdani-type FL (Ad_Mandani_FL), and the adaptive Sugeno-type FL (Ad_Sugeno_FL) for the simulated scenarios.

The optimized FL is the best option in 43% of the cases, but this does not mean it is the best option overall. Moreover, from Figure 17, a comparison has been performed, but only between the adaptive Sugeno FL and EMS5 EMSs. The adaptive Sugeno FL EMS is the best in 57% of the cases, while the GA-FL EMS is the best in 43% of the cases.

In addition, the distributions of the results have been analyzed seasonally. The results can be seen in Figure 18.

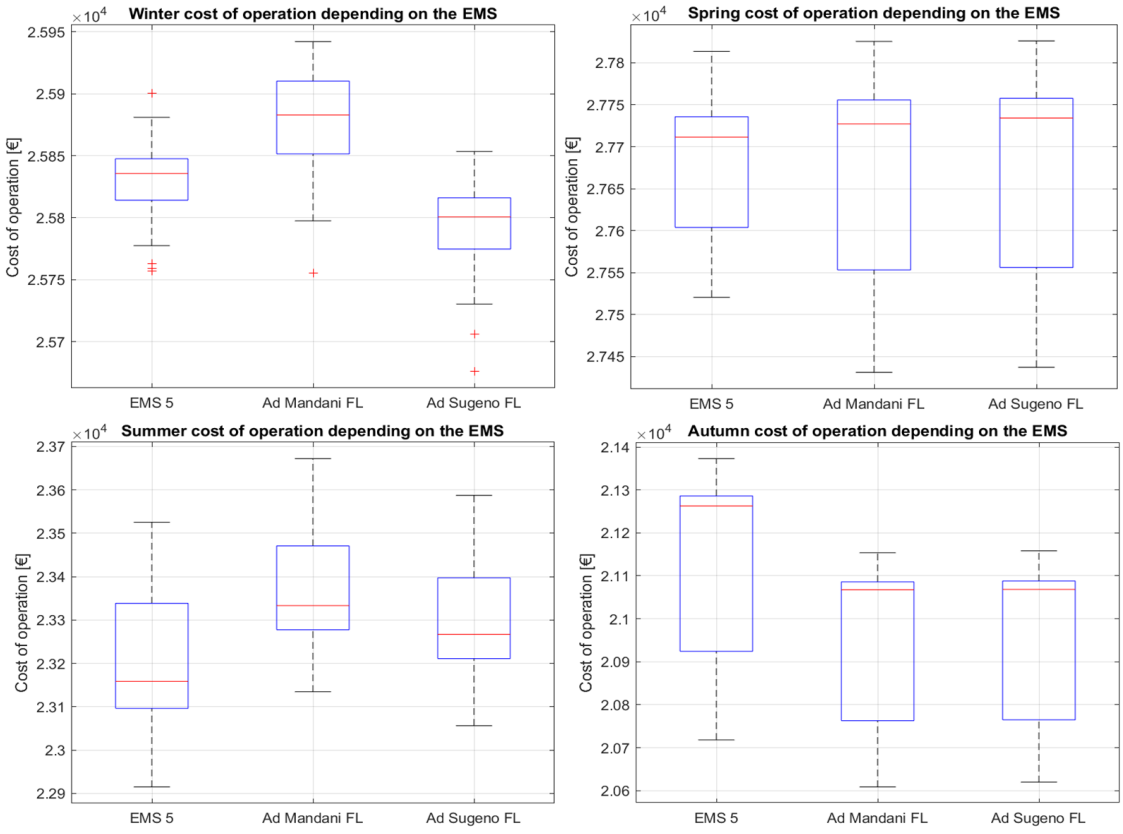

Figure 18. Distribution of operational price cost depending on the EMS and the season for the analyzed 30 different power profiles.

In these boxplots, the results of the best EMSs for the 30 different power load cases are shown seasonally separated. Each box shows the distribution of the 30 cases of each season's operational cost when that specific EMS is used.

Regarding the results between the adaptative Mandani and Sugeno FLs, the distributions of spring and autumn are almost identical, but the adaptive Sugeno FL is cheaper in summer and winter overall. Thus, the adaptive Sugeno FL is the better EMS of the two.

Regarding the results between the adaptive Sugeno FL and the EMS5, the conclusions are not so clear. The adaptive Sugeno FL performs better in autumn and winter, while the EMS5 is better in summer. In spring, the adaptive Sugeno FL results are distributed in a bigger range, while the EMS5 results are closer. The median of the results is slightly lower when the EMS5 is used, but the cheapest results of the adaptative Sugeno FL are cheaper than the ones of the EMS5.

The analysis presented in this section demonstrate that the optimized FL can be improved using an adaptive approach.

4. Conclusions

This work presents a comparative analysis of EMS strategies for EVCSs integrated with BESSs, based on a real urban bus fleet scenario. This study evaluates the impact of EMS design and seasonal electricity price variations on operating costs.

Optimizing the EV charging schedule using GAs alone results in cost savings of over 10%. When integrating BESSs, the adaptive fuzzy logic EMS enhanced with price forecasting showed the highest cost reduction, exceeding 15% annually.

Key factors behind this performance include the flexibility of fuzzy control and its ability to integrate forecast data for proactive decision-making.

Future work will assess the broader sustainability of the proposed solutions and investigate hybrid fuzzy–GA systems and learning-based EMSs for real-time applications. A unified optimization framework will also be developed to support diverse EVCS configurations.

Author Contributions: J.O.: Conceptualization, Methodology, Software, Formal analysis, Investigation, Writing—Original Draft, Writing—Review & Editing. H.C.: Validation, Writing—Original Draft, Writing—Review & Editing, Supervision. J.A.L.-I.: Conceptualization, Validation, Supervision. T.T.L.: Validation, Writing—Review & Editing. All authors have read and agreed to the published version of the manuscript.

Funding: This research received no external funding.

Institutional Review Board Statement: Not applicable.

Informed Consent Statement: Not applicable.

Data Availability Statement: Data related to this study are confidential.

Conflicts of Interest: Author Jon Ander López-Ibarra was employed by the company Jema Energy. The remaining authors declare that the research was conducted in the absence of any commercial or financial relationships that could be construed as a potential conflict of interest.

Nomenclature

Acronyms

AC	Alternating Current
BESS	Battery Energy Storage System
DC	Direct Current or Continuous Current
DOD	Depth of Discharge
EMS	Energy Management System
ESS	Energy Storage System
EV	Electric Vehicle
EVCS	Electric Vehicle Charging Station
FL	Fuzzy Logic
GA	Genetic Algorithm
GHG	Greenhouse Gas
MF	Membership Function
RB	Rule-Based
ROI	Return of Investment
SOC	State of Charge

Appendix A

Original Charging Schedule of the Studied Case Study EVCS

The original charging strategy of the analyzed specific EVCS can be seen in Figure A1. The horizontal axis represents each bus, so there are 89 columns. The vertical axis represents the hour of the day, with an interval of 15 min, so there are 96 lines. The blue in (X, Y) indicates that bus X is on the move at time Y, so it cannot be charged. The green in (X, Y) indicates that bus X is being charged at 60 kW during time Y. The red color in (X, Y) indicates that bus X is being charged at 120 kW during time Y. The white color in (X, Y) indicates that bus X is in the depot at time Y, so it is possible to charge the bus at this time.

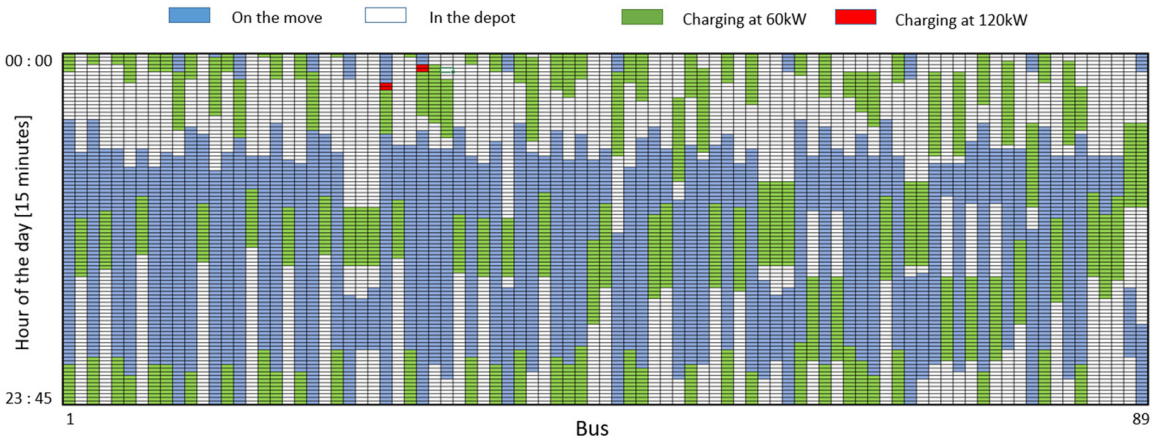

Figure A1. Original charging schedule of the analysed case study.

References

1. World Resources Institute. World Greenhouse Gas Emissions. 2019. Available online: https://www.wri.org/data/world-greenhouse-gas-emissions-2019 (accessed on 29 January 2024).
2. Serrano, J.R.; Novella, R.; Piqueras, P. Why the development of internal combustion engines is still necessary to fight against global climate change from the perspective of transportation. *Appl. Sci.* **2019**, *9*, 4597. [CrossRef]
3. Huang, Q.; Yang, L.; Zhou, C.; Luo, L.; Wang, P. Pricing and energy management of EV charging station with distributed renewable energy and storage. *Energy* **2023**, *9*, 289–295. [CrossRef]
4. Parlikar, A.; Schott, M.; Godse, K.; Kucevic, D.; Jossen, A.; Hesse, H. High-power electric vehicle charging: Low-carbon grid integration pathways with stationary lithium-ion battery systems and renewable generation. *Appl. Energy* **2023**, *333*, 120541. [CrossRef]
5. Li, D.; Zouma, A.; Liao, J.; Yang, H. An energy management strategy with renewable energy and energy storage system for a large electric vehicle charging station. *eTransportation* **2020**, *6*, 100076. [CrossRef]
6. Yan, Y.; Wang, H.; Jiang, J.; Zhang, W.; Bao, Y.; Huang, M. Research on configuration methods of battery energy storage system for pure electric bus fast charging station. *Energies* **2019**, *12*, 558. [CrossRef]
7. Zhao, C.; Andersen, P.B.; Træholt, C.; Hashemi, S. Grid-connected battery energy storage system: A review on application and integration. *Renew. Sustain. Energy Rev.* **2023**, *182*, 113400. [CrossRef]
8. Karkuzhali, S.; Rani, P.U. Examination on Classification of EVs and Energy Management Strategies of HEV. *Int. J. Innov. Technol. Explor. Eng.* **2019**, *9* (Suppl. S1), 261–266. [CrossRef]
9. Wu, Y.; Ravey, A.; Chrenko, D.; Miraoui, A. Demand Side Energy Management of EV Charging Stations by Approximate Dynamic Programming. *Energy Convers. Manag.* **2019**, *196*, 878–890. [CrossRef]
10. Mateen, S. Discrete Stochastic Control for Energy Management with Photovoltaic Electric Vehicle Charging Station. *CPSS Trans. Power Electron. Appl.* **2022**, *7*, 216–225. [CrossRef]
11. Glover, F.; Laguna, M.; Martí, R.; Glover, A. Fundamentals of Scatter Search and Path Relinking. *Control Cybern.* **2000**, *29*, 653–684.
12. Ganesh, A.H.; Xu, B. A review of reinforcement learning based energy management systems for electrified powertrains: Progress, challenge, and potential solution. *Renew. Sustain. Energy Rev.* **2022**, *154*, 111833. [CrossRef]
13. Torkan, R.; Ilinca, A.; Ghorbanzadeh, M. A genetic algorithm approach for smart energy management of microgrids. *Renew. Energy* **2022**, *197*, 852–863. [CrossRef]
14. Wang, F.Y.; Chen, Z.; Hu, Z. Comprehensive optimization of electrical heacy-duty truck battery swap stations with a SOC-dependant charge scheduling method. *Energy* **2024**, *308*, 132773. [CrossRef]
15. Jeon, M.; Tong, L.; Zhao, Q. On the Optimality of Procrastination Policy for EV charging under Net Energy Metering. *arXiv* **2023**, arXiv:2304.04076. [CrossRef]
16. Basma, H.; Mansour, C.; Haddad, M.; Nemer, M.; Stabat, P. A novel method for co-optiimzing battery sizing and charging strategy of battery electric bus flets: An application to the city of Paris. *Energy* **2023**, *285*, 129459. [CrossRef]
17. Hosny, M.; Mumford, C. Investigating Genetic Algorithms for Solving the Multiple Vehicle Pickup and Delivery Problem with Time Windows. In Proceedings of the MIC2009, the VIII Metaheuristics International Conference, Hamburg, Germany, 13–16 June 2009.
18. Sun, B.; Huang, Z.; Tan, X.; Tsang, D.H.K. Optimal scheduling for electric vehicle charging with discrete charging levels in distribution grid. *IEEE Trans. Smart Grid* **2018**, *9*, 624–634. [CrossRef]

19. Abdullah, H.M.; Gastli, A.; Ben-Brahim, L. Reinforcement Learning Based EV Charging Management Systems-A Review. *IEEE Access* **2021**, *9*, 41506–41531. [CrossRef]
20. Rafał, K.; Radziszewska, W.; Grabowski, O.; Biedka, H.; Verstraete, J. Energy Cost Minimization with Hybrid Energy Storage System Using Optimization Algorithm. *Appl. Sci.* **2023**, *13*, 518. [CrossRef]
21. Lee, J.O.; Kim, Y.S. Novel battery degradation cost formulation for optimal scheduling of battery energy storage systems. *Int. J. Electr. Power Energy Syst.* **2022**, *137*, 107795. [CrossRef]
22. Chaudhari, K.; Ukil, A.; Kumar, K.N.; Manandhar, U.; Kollimalla, S.K. Hybrid Optimization for Economic Deployment of ESS in PV-Integrated EV Charging Stations. *IEEE Trans. Ind. Inf.* **2018**, *14*, 106–116. [CrossRef]
23. Yang, J.; Yu, F.; Ma, K.; Yang, B.; Yue, Z. Optimal scheduling of electric-hydrogen integrated charging station for new energy vehicles. *Renew. Energy* **2024**, *224*, 120224. [CrossRef]
24. Gauthier, R.; Luscombe, A.; Bond, T.; Bauer, M.; Johnson, M.; Harlow, J.; Louli, A.; Dahn, J.R. How do Depth of Discharge, C-rate and Calendar Age Affect Capacity Retention, Impedance Growth, the Electrodes, and the Electrolyte in Li-Ion Cells? *J. Electrochem. Soc.* **2022**, *169*, 020518. [CrossRef]
25. Herrera, V.; Milo, A.; Gaztañaga, H.; Etxebarria-Otadui, I.; Villareal, I.; Camblong, H. Adaptative energy management strategy and optimal sizing applied on a battery-supercapacitor based tramway. *Appl. Energy* **2016**, *169*, 831–845. [CrossRef]
26. De Santis, E.; Rizzi, A.; Sadeghian, A. A Hierarchical Genetic Optimization of a Fuzzy Logic System for Flow Control in Micro Grids. *arXiv* **2016**, arXiv:1604.04789. [CrossRef]
27. Patil, V.P.; Pawar, D.D. The Optimal Crossover or Mutation Rates in Genetic Algorithm: A Review. *Int. J. Appl. Eng. Technol.* **2015**, *5*, 38–41.
28. Wu, C.-J.; Liu, G.-Y. A Genetic Approach for Simultaneous Design of Membership Functions and Fuzzy Control Rules. *J. Intell. Robot. Syst.* **2000**, *28*, 195–211. [CrossRef]
29. Polat, H.; Hosseinabadi, F.; Hasan, M.; Chakraborty, S.; Geury, T.; El Baghdadi, M.; Wilkins, S.; Hegazy, O. A Review of DC Fast Chargers with BESS for Electric Vehicles: Topology, Battery, Reliability Oriented Control and Cooling Perspectives. *Batteries* **2023**, *9*, 121. [CrossRef]
30. OMIE Webpage. Available online: https://www.omie.es/es (accessed on 29 January 2024).
31. Mauler, L.; Duffner, F.; Zeier, W.G.; Leker, J. Battery cost forecasting: A review of methods and results with an outlook to 2050. *Energy Environ. Sci.* **2021**, *14*, 4712–4739. [CrossRef]